A posteriori estimation of dimension reduction errors for elliptic problems on thin domains

Repin, S ; Sauter, S ; Smolianski, A

DOI: https://doi.org/10.1137/030602381

SIAM J. NUMER. ANAL.
Vol. 42, No. 4, pp. 1435–1451

A POSTERIORI ESTIMATION OF DIMENSION REDUCTION ERRORS FOR ELLIPTIC PROBLEMS ON THIN DOMAINS*

SERGEY REPIN†, STEFAN SAUTER‡, AND ANTON SMOLIANSKI‡

Abstract. A new a posteriori error estimator is presented for the verification of the dimensionally reduced models stemming from the elliptic problems on thin domains. The original problem is considered in a general setting, without any specific assumptions on the domain geometry, coefficients, and the right-hand sides. For the energy norm of the error of the zero-order dimension reduction method, the proposed estimator is shown to always provide a guaranteed upper bound. In the case when the original domain has constant thickness (but, possibly, nonplane upper and lower faces), the estimator demonstrates the optimal convergence rate as the thickness tends to zero. It is also flexible enough to successfully cope with infinitely growing right-hand sides in the equation when the domain thickness tends to zero. The numerical tests indicate the efficiency of the estimator and its ability to accurately represent the local error distribution needed for an adaptive improvement of the reduced model.

Key words. dimension reduction, thin domain, a posteriori error estimate, reliability, efficiency, local error distribution

AMS subject classifications. 35J20, 65N15, 65N30

DOI. 10.1137/030602381

1. Introduction.

The method of dimension reduction is a popular approach frequently used by engineers for the approximate solution of the problems posed in *thin* domains. The term "thin" means that the size of the original physical domain along one coordinate direction is much smaller than along the others; this allows us to make some simplifying assumptions on the behavior of the exact solution and to replace the original high-dimensional problem with a lower-dimensional one. For instance, such a situation arises if a three-dimensional problem is analyzed with the help of a two-dimensional model. It is, however, clear that the solution of the new, "reduced" problem will, in general, differ from the solution to the original high-dimensional problem. Thus, the dimension reduction method unavoidably produces an error that can be referred to as the dimension reduction or the *modeling error*. The essential part of the model verification is, hence, a reliable *a posteriori* control of the dimension reduction error.

Despite the practical importance of the topic, only a few a posteriori estimators for the dimension reduction error have been introduced so far. In [15] and [3] (see also [2]) the residual-type estimators were proposed and proved reliable and efficient under the assumptions that the right-hand side of the given equation is zero and the original domain is a plate with plane parallel faces. In [5] and [12] the implicit estimators based on the solution of local three-dimensional Neumann problems were developed for the hierarchical modeling of complex elastic plates. In [1] the estimator of Babuška and Schwab (see [2], [3]) was extended to take into account the discretization error stemming from the approximate solution of the reduced problem. In this respect, we

*Received by the editors May 5, 2004; accepted for publication (in revised form) May 13, 2004; published electronically December 16, 2004.
http://www.siam.org/journals/sinum/42-4/60238.html
†V. A. Steklov Institute of Mathematics, Fontanka 27, 191 011 St. Petersburg, Russia (repin@pdmi.ras.ru).
‡Institute of Mathematics, Zurich University, Winterthurerstrasse 190, CH-8057 Zurich, Switzerland (stas@amath.unizh.ch, antsmol@amath.unizh.ch).

have to notice that the present work is focused on the estimation of the modeling error; i.e., we assume, exactly as in [2], [3], that the error of discretizing the reduced problem is negligible. The work on the simultaneous a posteriori estimation of both the modeling error and the discretization error will be reported in a forthcoming paper.

In this work we propose a reliable and efficient a posteriori estimator for the dimension reduction error in the energy norm, having no specific assumptions on the right-hand side of the given equation and considering a general geometry of the given domain. In contrast to the above-mentioned papers, which deal with the hierarchical modeling of the problems in thin domains, we consider only the so-called *zero-order method* of dimension reduction that is, however, very popular owing to its simplicity and purely two-dimensional formulation. At the same time, this method forms a basis for the hierarchical modeling of three-dimensional plates (see, e.g., [14], [3], [12]). It is also worth noting that the zero-order method of dimension reduction does not cover the important Kirchhoff plate model in linear elasticity. The presented approach can, however, be extended to this case; the work on this subject is underway.

We advocate the functional-type a posteriori error estimation approach (see [7], [8], [9], [10]) that essentially differs from the approaches taken in the aforementioned articles; however, surprisingly enough, it is possible to show that Babuška and Schwab's estimator for the zero-order reduced problem can be obtained as a particular case of our estimator when the right-hand side of the equation is zero and the original domain is a plate with plane parallel faces. It must also be noticed that the treatment of the case with nonzero right-hand side may require special care, as we are about to see in one of the numerical examples; the presented estimator exhibits sufficient flexibility to remain efficient in this case.

The paper is set out as follows. Section 2 contains the geometric definitions and the problem statement. In section 3 we derive the reduced problem. Section 4 is devoted to the derivation of the a posteriori error estimate, while in section 5 we consider two particular cases and analyze the behavior of the estimator. The numerical examples are considered in section 6, and we draw the conclusions in section 7.

2. Problem setting. We consider three-dimensional Lipschitz domains, which can be given in the form

$$\Omega := \{x \in \mathbb{R}^3 \mid (x_1, x_2) \in \widehat{\Omega}\,,\ d_\ominus(x_1, x_2) < x_3 < d_\oplus(x_1, x_2)\}\,,$$

where $\widehat{\Omega} \subset \mathbb{R}^2$ is the orthogonal projection of Ω on the (x_1, x_2)-plane ($\widehat{\Omega}$ has the Lipschitz boundary $\widehat{\Gamma}$) and $d_\ominus$ and $d_\oplus$ are Lipschitz continuous functions defined on $\overline{\widehat{\Omega}}$. The lower and upper faces of Ω are denoted by

$$\Gamma_\ominus := \{x \in \mathbb{R}^3 \mid (x_1, x_2) \in \widehat{\Omega}\,,\ x_3 = d_\ominus(x_1, x_2)\}$$

and

$$\Gamma_\oplus := \{x \in \mathbb{R}^3 \mid (x_1, x_2) \in \widehat{\Omega}\,,\ x_3 = d_\oplus(x_1, x_2)\}\,;$$

the lateral boundary by

$$\Gamma_0 := \{x \in \mathbb{R}^3 \mid (x_1, x_2) \in \widehat{\Gamma}\,,\ d_\ominus(x_1, x_2) < x_3 < d_\oplus(x_1, x_2)\}$$

(see Figure 1).

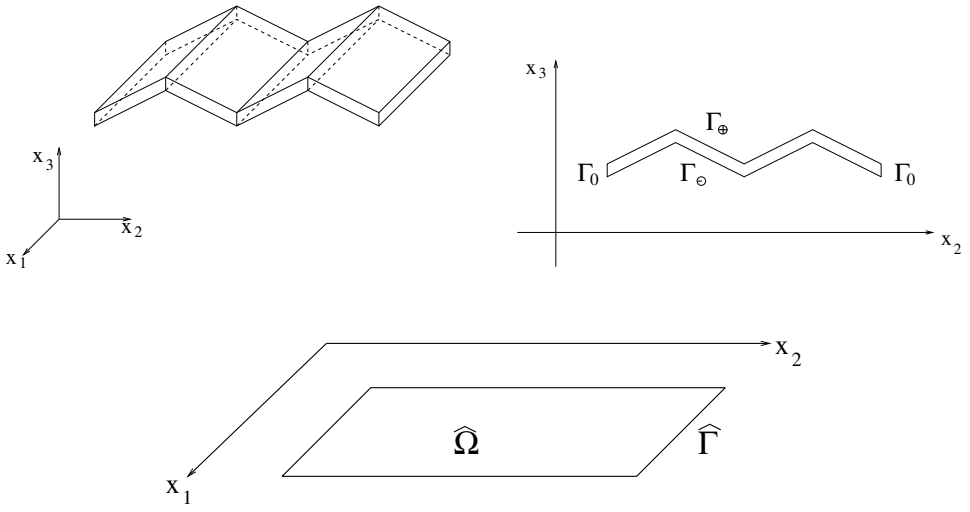

FIG. 1. *Sketch of the domain geometry.*

Remark 2.1. We consider $d_\ominus$ and $d_\oplus$ as explicit functions of (x_1, x_2)-coordinates only for the sake of simplicity. The generalization of the theory to the case of an arbitrary Lipschitz domain Ω presents no difficulty from the conceptional point of view.

The assumption that the given domain Ω is "thin" can now be written as

$$\operatorname{diam}\widehat{\Omega} \gg \max_{(x_1,x_2)\in\overline{\widehat{\Omega}}} d\,(x_1, x_2)\,, \tag{2.1}$$

where $d = d_\oplus - d_\ominus$ is the domain thickness, $d\,(x_1, x_2) \geq d_* > 0 \;\; \forall (x_1, x_2) \in \overline{\widehat{\Omega}}$. Although the assumption is of a purely qualitative nature, it will motivate the derivation of the corresponding two-dimensional reduced model in the next section. We also have to notice that Figure 1 depicts a simplified case; in the geometrical definitions we do not assume the domain thickness $d\,(x_1, x_2)$ to be a constant.

In the domain Ω we consider a model elliptic problem

$$-\operatorname{Div}(\mathbf{A}\nabla u) = f \quad \text{in } \Omega\,, \tag{2.2}$$

$$u = 0 \quad \text{on } \Gamma_0\,, \tag{2.3}$$

$$\mathbf{A}\nabla u \cdot \boldsymbol{\nu}_\ominus = F_\ominus \text{ on } \Gamma_\ominus\,, \tag{2.4}$$

$$\mathbf{A}\nabla u \cdot \boldsymbol{\nu}_\oplus = F_\oplus \text{ on } \Gamma_\oplus\,, \tag{2.5}$$

where $f \in L_2(\Omega)$, $F_\ominus \in L_2(\Gamma_\ominus)$, $F_\oplus \in L_2(\Gamma_\oplus)$, and $\boldsymbol{\nu}_\ominus$ and $\boldsymbol{\nu}_\oplus$ are outward normal vectors at $\Gamma_\ominus$ and $\Gamma_\oplus$, respectively. The matrix $\mathbf{A} = (a_{ij}(x))_{i,j=\overline{1,3}}$ with the components from $L_\infty(\Omega)$ is symmetric and uniformly positive definite; i.e., there exist constants $0 < c < C < \infty$ such that

$$c|\xi|^2 \leq \mathbf{A}(x)\xi \cdot \xi \leq C|\xi|^2 \quad \forall \xi \in \mathbb{R}^3, \text{ a.e. in } \Omega. \tag{2.6}$$

If the space of admissible functions is denoted by

$$V_0 := \{v \in H^1(\Omega) \mid v = 0 \text{ on } \Gamma_0\}\,, \tag{2.7}$$

the weak form of problem (2.2)–(2.5) reads as follows.

Problem (P). Find $u \in V_0$ such that

$$\int_\Omega \mathbf{A}\nabla u \cdot \nabla w \, dx = \int_\Omega f\, w \, dx + \int_{\Gamma_\ominus} F_\ominus \, w \, ds + \int_{\Gamma_\oplus} F_\oplus \, w \, ds \qquad \forall w \in V_0 \,. \tag{2.8}$$

From now on we will frequently use the notation $\widehat{x} = (x_1, x_2)$, $\widehat{x} \in \widehat{\Omega}$, and all functions depending only on (x_1, x_2) will be marked by $\widehat{\ }$; in addition, we will distinguish between the three- and two-dimensional divergence operators:

$$\mathrm{Div}\, \boldsymbol{\tau} = \frac{\partial \boldsymbol{\tau}_1}{\partial x_1} + \frac{\partial \boldsymbol{\tau}_2}{\partial x_2} + \frac{\partial \boldsymbol{\tau}_3}{\partial x_3} \,, \quad \mathrm{div}\, \widehat{\boldsymbol{\tau}} = \frac{\partial \widehat{\boldsymbol{\tau}}_1}{\partial x_1} + \frac{\partial \widehat{\boldsymbol{\tau}}_2}{\partial x_2} \,.$$

We also denote $\widehat{F}_\ominus(\widehat{x}) := F_\ominus(\widehat{x}, d_\ominus(\widehat{x}))$, $\widehat{F}_\oplus(\widehat{x}) := F_\oplus(\widehat{x}, d_\oplus(\widehat{x}))$ for any $\widehat{x} \in \widehat{\Omega}$. Finally, we define the energy norm

$$|||v||| := \left(\int_\Omega \mathbf{A}(x) \nabla v \cdot \nabla v \, dx \right)^{1/2} \qquad \forall v \in V_0 \,. \tag{2.9}$$

3. The reduced problem. In view of (2.1), it is reasonable to consider the hypothesis that

(3.1) the exact solution u is almost *constant* with respect to the x_3-coordinate.

This gives rise to the so-called *zero-order reduced model* for the original problem (2.8). The model is very popular due to its simplicity and purely two-dimensional formulation. A discussion on the hierarchy of reduced models of different orders can be found in, e.g., [14], [3].

With (3.1) in mind, one can expect that the exact solution u may be well approximated by the functions from the subspace

(3.2)
$$\widehat{V}_0 := \{ v \in V_0 \mid \exists\, \widehat{v} \in H^1_0(\widehat{\Omega}) \ \text{ such that } \ v(x) = \widehat{v}(\widehat{x}) \ \text{ for a.e. } \ x = (\widehat{x}, x_3) \in \Omega \} \,.$$

Thus, any function from $\widehat{V}_0$ can be identified with the corresponding function $\widehat{v} \in H^1_0(\widehat{\Omega})$ (and vice versa: for any $\widehat{v} \in H^1_0(\widehat{\Omega})$ one can reconstruct $v \in \widehat{V}_0 \subset V_0$ by the constant extension as in the definition of $\widehat{V}_0$). Then, the energy-norm projection of u onto the subspace $\widehat{V}_0$ yields the following *reduced problem* (the zero-order reduced model).

Problem ($\widehat{P}$). Find $\widehat{u} \in \widehat{V}_0$ such that

$$\int_\Omega \mathbf{A}\nabla \widehat{u} \cdot \nabla \widehat{w} \, dx = \int_\Omega f\, \widehat{w} \, dx + \int_{\Gamma_\ominus} F_\ominus \, \widehat{w} \, ds + \int_{\Gamma_\oplus} F_\oplus \, \widehat{w} \, ds \qquad \forall \widehat{w} \in \widehat{V}_0 \,. \tag{3.3}$$

Now we can define the dimension reduction error (the *modeling error*) as the difference $e := u - \widehat{u}$ between the solution to the original problem (2.8) and the solution to the reduced problem (3.3).

Remark 3.1. It may be noticed that assumption (2.1) (and, consequently, (3.1)) serves only as an intuitive motivation for the introduction of the approximation subspace $\widehat{V}_0$ and the reduced problem (3.3). Since the assumption cannot be quantified,

the real error of "replacing" u with $\widehat{u}$ may be large; a robust a posteriori error estimator should, however, measure this error sufficiently accurately even in the cases when assumption (2.1) is virtually unsatisfied.

Remark 3.2. The asymptotic behavior of the modeling error e was analyzed in [14] (see also [2]) for the case of a plate with plane parallel faces $\Gamma_\ominus$ and $\Gamma_\oplus$ (i.e., when $d_\ominus = -\frac{d_0}{2}$, $d_\oplus = \frac{d_0}{2}$, $d_0 = \text{const} > 0$ is the plate thickness) and $f = 0$. It was proved that

$$|||e||| \le C\, d_0^{1/2} \left(\|\widehat{F}_\ominus\|_{L_2(\widehat{\Omega})} + \|\widehat{F}_\oplus\|_{L_2(\widehat{\Omega})} \right) \quad \text{as } d_0 \to 0\,.$$

Remark 3.3. We have to note that the third component of the vector $\nabla\widehat{u}$ is zero (since $\widehat{u}$ does not depend on x_3) and, thus, the vector will sometimes be considered as a two-component vector when no confusion is possible.

In order to see that the reduced problem (3.3) is, in fact, a two-dimensional problem, we define the operation $(\widetilde{\ })$ of averaging in the x_3-direction as follows:

$$\forall g \in L_1(\Omega) : \quad \widetilde{g}(\widehat{x}) := \frac{1}{d\,(\widehat{x})} \int_{d_\ominus(\widehat{x})}^{d_\oplus(\widehat{x})} g(\widehat{x}, x_3)\, dx_3 \ \text{ for a.e. } \widehat{x} \in \widehat{\Omega}\,,$$

and, having noticed that

$$\int_{\Gamma_\ominus} F_\ominus\, \widehat{w}\, ds = \int_{\widehat{\Omega}} \widehat{F}_\ominus\,(\widehat{x})\, \widehat{w}\,(\widehat{x}) \sqrt{1 + |\nabla d_\ominus(\widehat{x})|^2}\, d\widehat{x} \quad \left(\text{analogously for } \int_{\Gamma_\oplus} F_\oplus\, \widehat{w}\, ds \right),$$

we can rewrite problem (3.3) as follows.

Find $\widehat{u} \in \widehat{V}_0$ such that

$$\int_{\widehat{\Omega}} d\,(\widehat{x}) \widetilde{\mathbf{A}}_p(\widehat{x}) \nabla\widehat{u} \cdot \nabla\widehat{w}\, d\widehat{x} = \int_{\widehat{\Omega}} d\,(\widehat{x}) \widehat{f}(\widehat{x}) \widehat{w}\, d\widehat{x} \quad \forall \widehat{w} \in \widehat{V}_0\,. \tag{3.4}$$

Here $\widetilde{\mathbf{A}}_p(\widehat{x}) = (\widetilde{a}_{ij}(\widehat{x}))_{i,j=\overline{1,2}}$ is the averaged "plane" part $\mathbf{A}_p(x)$ $(\mathbf{A}_p(x) = (a_{ij}(x))_{i,j=\overline{1,2}})$ of the matrix $\mathbf{A}$ and

$$\widehat{f}(\widehat{x}) = \widetilde{f}(\widehat{x}) + \frac{\widehat{F}_\ominus(\widehat{x}) \sqrt{1 + |\nabla d_\ominus(\widehat{x})|^2} + \widehat{F}_\oplus(\widehat{x}) \sqrt{1 + |\nabla d_\oplus(\widehat{x})|^2}}{d\,(\widehat{x})}\,.$$

It is clear that problem (3.4) is a two-dimensional elliptic problem with the homogeneous Dirichlet boundary condition

$$-\mathrm{div}\,(d(\widehat{x})\, \widetilde{\mathbf{A}}_p(\widehat{x}) \nabla\widehat{u}) = d(\widehat{x})\, \widehat{f}(\widehat{x}) \quad \text{in } \widehat{\Omega}, \tag{3.5}$$

$$\widehat{u} = 0 \quad \text{on } \widehat{\Gamma}\,. \tag{3.6}$$

4. A posteriori estimation of the modeling error. In order to control the dimension reduction error, we apply the functional-type a posteriori error estimate derived in [10] (see also [7] and [9]) to the original three-dimensional problem (2.8). The estimate reads as follows.

For all $\gamma > 0$, $\delta > 0$, and $y^* \in H_*(\Omega, \mathrm{Div})$ there holds

$$\begin{aligned} |||u - v|||^2 \le{}& (1+\gamma)\, M_1^2\,(v, y^*) + \left(1 + \frac{1}{\gamma}\right)(1+\delta)\, C_\Omega^2\, M_2^2\,(y^*) \\ &+ \left(1 + \frac{1}{\gamma}\right)\left(1 + \frac{1}{\delta}\right) C_\Gamma^2 (1 + C_\Omega^2)\, M_3^2\,(y^*), \end{aligned} \tag{4.1}$$

where v is any function from the energy space V_0, C_Ω is the constant from Friedrichs' inequality,

$$C_\Omega^{-2} = \inf_{w \in V_0 \setminus \{0\}} \frac{|||w|||^2}{\|w\|^2_{L_2(\Omega)}}\,, \tag{4.2}$$

C_Γ is the constant from the trace inequality,

$$C_\Gamma^2 = \sup_{w \in V_0 \setminus \{0\}} \frac{\|w\|^2_{L_2(\Gamma_\oplus)} + \|w\|^2_{L_2(\Gamma_\ominus)}}{|||w|||^2 + \|w\|^2_{L_2(\Omega)}}\,, \tag{4.3}$$

the space $H_*(\Omega, \mathrm{Div})$ is defined as

$$H_*(\Omega, \mathrm{Div}) := \{y^* \in L_2(\Omega, \mathbb{R}^3) \mid \mathrm{Div}\, y^* \in L_2(\Omega)\,,\ y^* \cdot \boldsymbol{\nu}_\ominus \in L_2(\Gamma_\ominus)\,,\ y^* \cdot \boldsymbol{\nu}_\oplus \in L_2(\Gamma_\oplus)\}\,,$$

and the functionals $M_1^2\,(v, y^*)$, $M_2^2\,(y^*)$, $M_3^2\,(y^*)$ are defined by

$$\begin{aligned}
M_1^2\,(v, y^*) &:= \int_\Omega (\nabla v - \mathbf{A}^{-1} y^*) \cdot (\mathbf{A}\nabla v - y^*)\, dx\,,\\
M_2^2\,(y^*) &:= \|\mathrm{Div}\, y^* + f\|^2_{L_2(\Omega)}\,,\\
M_3^2\,(y^*) &:= \|F_\ominus - y^* \cdot \boldsymbol{\nu}_\ominus\|^2_{L_2(\Gamma_\ominus)} + \|F_\oplus - y^* \cdot \boldsymbol{\nu}_\oplus\|^2_{L_2(\Gamma_\oplus)}\,.
\end{aligned}$$

In what follows, we will denote the functionals simply by M_1^2, M_2^2, M_3^2. Since estimate (4.1) holds true for any "approximate solution" v from V_0 and since the solution $\widehat{u}$ of the reduced problem is in $\widehat{V}_0 \subset V_0$, we can simply plug $\widehat{u}$ into estimate (4.1) to obtain an upper bound of the modeling error. We also emphasize that the estimate is valid for any positive numbers γ and δ and for any vector-function y^* from the space $H_*(\Omega, \mathrm{Div})$. While the best possible option would be to take as y^* the exact flux $\mathbf{A}\nabla u$ (then M_2 and M_3 would vanish and M_1 would give us the energy norm of the exact error), we have to restrict ourselves to choosing some computable quantity, i.e., not containing the unknown exact solution u. We approximate the flux by

$$y^* = \widetilde{\mathbf{A}}_p \nabla \widehat{u} + \boldsymbol{\tau}^*\,, \tag{4.4}$$

with $\boldsymbol{\tau}^* = \{0\,,\ 0\,,\ \psi(x)\}^T$. Here ψ is the auxiliary function from $L_2(\Omega)$ satisfying the conditions $\frac{\partial \psi}{\partial x_3} \in L_2(\Omega)\,$, $\psi \in L_2(\Gamma_\ominus)$, and $\psi \in L_2(\Gamma_\oplus)$. The concrete form of the function ψ will be given later. Its meaning becomes clear in the case of the Poisson equation (i.e., if $\mathbf{A}$ is the identity matrix), where ψ should, obviously, approximate the derivative $\frac{\partial u}{\partial x_3}$ of the exact solution in the x_3-direction. Using (3.5), it is easy to verify that y^* from (4.4) belongs to $H_*(\Omega, \mathrm{Div})$.

Remark 4.1. If in (4.1) we take y^* from the set

$$Q^*_{f,F} := \{q^* \in L_2(\Omega, \mathbb{R}^3) \mid \mathrm{Div}\, q^* = -f \text{ in } \Omega\,,\ q^* \cdot \boldsymbol{\nu}_{\ominus,\oplus} = F_{\ominus,\oplus} \text{ on } \Gamma_{\ominus,\oplus}\}\,,$$

we obtain the dual-formulation-based error estimate of [4] (see also [6] and [13]). Since it is not easy to satisfy the constraints of the set $Q^*_{f,F}$, the estimate (4.1) with y^* from $H_*(\Omega, \mathrm{Div})$ seems to be more practical. In particular, for the estimation of the modeling error under consideration we essentially exploit the freedom of choosing y^* in the whole space $H_*(\Omega, \mathrm{Div})$.

Remark 4.2. The estimate (4.1) possesses the property of asymptotic exactness (see [10]) but, if we choose y^* as in (4.4), this property might be lost, since the

only remaining "degree of freedom" is the function ψ and the approximate plane flux $\widetilde{\mathbf{A}}_p\nabla\widehat{u}$ may not sufficiently represent the first two components of the exact flux $\mathbf{A}\nabla u$. On the other hand, if we did not fix the first two components of y^*, the process of estimation would require the minimization of the right-hand side of (4.1) with respect to those components, which is, in principle, equivalent to solving a three-dimensional problem. However, our goal is to avoid any truly three-dimensional calculations in the evaluation of the error estimator (this process should not be more expensive than the solution of the reduced problem). Fortunately, in most of the situations, $\widetilde{\mathbf{A}}_p\nabla\widehat{u}$ is a good approximation to the "plane" part of the exact flux, and the modeling-error estimate with y^* as in (4.4) exhibits both efficiency and flexibility, as the numerical tests of section 6 show.

In order to rewrite estimate (4.1) in a more convenient form, we introduce the notation

$$\mathbf{B} := \mathbf{A}^{-1} \quad (\mathbf{B}(x) = (b_{ij}(x))_{i,j=\overline{1,3}}\,,\ \ \mathbf{B} = \mathbf{B}^T)\,, \tag{4.5}$$

$$\mathbf{B}_p := (b_{ij})_{i,j=\overline{1,2}}\,, \tag{4.6}$$

$$\mathbf{b}_3 := \{b_{31}\,,\ b_{32}\}^T\,. \tag{4.7}$$

The term M_1^2 with $v = \widehat{u}$ reads

$$M_1^2 = \int_\Omega (\nabla\widehat{u} - \mathbf{B}y^*)\cdot(\mathbf{A}\nabla\widehat{u} - y^*)\,dx = \int_\Omega (\mathbf{A}\nabla\widehat{u}\cdot\nabla\widehat{u} - 2y^*\cdot\nabla\widehat{u} + \mathbf{B}y^*\cdot y^*)\,dx\,. \tag{4.8}$$

For the first term in (4.8), one immediately obtains

$$\int_\Omega \mathbf{A}\nabla\widehat{u}\cdot\nabla\widehat{u}\,dx = \int_{\widehat{\Omega}} d\,(\widehat{x})\widetilde{\mathbf{A}}_p(\widehat{x})\nabla\widehat{u}\cdot\nabla\widehat{u}\,d\widehat{x}\,. \tag{4.9}$$

The second term in (4.8) can be further rewritten if one notices that (recall $\frac{\partial\widehat{u}}{\partial x_3} = 0$)

$$y^*\cdot\nabla\widehat{u} = (\widetilde{\mathbf{A}}_p\nabla\widehat{u} + \tau^*)\cdot\nabla\widehat{u} = \widetilde{\mathbf{A}}_p\nabla\widehat{u}\cdot\nabla\widehat{u}\,.$$

Thus,

$$\int_\Omega y^*\cdot\nabla\widehat{u}\,dx = \int_{\widehat{\Omega}} d\,(\widehat{x})\widetilde{\mathbf{A}}_p(\widehat{x})\nabla\widehat{u}\cdot\nabla\widehat{u}\,d\widehat{x}\,. \tag{4.10}$$

For the third term in (4.8) we have

$$\begin{aligned}\mathbf{B}y^*\cdot y^* &= (\mathbf{B}\widetilde{\mathbf{A}}_p\nabla\widehat{u} + \mathbf{B}\tau^*)\cdot(\widetilde{\mathbf{A}}_p\nabla\widehat{u} + \tau^*) = \mathbf{B}\widetilde{\mathbf{A}}_p\nabla\widehat{u}\cdot\widetilde{\mathbf{A}}_p\nabla\widehat{u} + \mathbf{B}\widetilde{\mathbf{A}}_p\nabla\widehat{u}\cdot\tau^*\\ &\quad + \mathbf{B}\tau^*\cdot\widetilde{\mathbf{A}}_p\nabla\widehat{u} + \mathbf{B}\tau^*\cdot\tau^* = \mathbf{B}_p\widetilde{\mathbf{A}}_p\nabla\widehat{u}\cdot\widetilde{\mathbf{A}}_p\nabla\widehat{u} + 2(\mathbf{b}_3\cdot\widetilde{\mathbf{A}}_p\nabla\widehat{u})\psi + b_{33}\psi^2\end{aligned}$$

that yields

$$\int_\Omega \mathbf{B}y^*\cdot y^*\,dx = \int_{\widehat{\Omega}} d\,(\widehat{x})\widetilde{\mathbf{B}}_p\widetilde{\mathbf{A}}_p\nabla\widehat{u}\cdot\widetilde{\mathbf{A}}_p\nabla\widehat{u}\,d\widehat{x} + \int_\Omega (b_{33}\psi(x)^2 + 2(\mathbf{b}_3\cdot\widetilde{\mathbf{A}}_p\nabla\widehat{u})\psi(x))\,dx\,, \tag{4.11}$$

where $\widetilde{\mathbf{B}}_p$ is the averaged "plane" part $\mathbf{B}_p(x)$ of the matrix $\mathbf{B}(x)$.

Substituting (4.9), (4.10), and (4.11) into (4.8), one obtains

(4.12)
$$M_1^2 = \int_{\widehat{\Omega}} d\,(\widehat{x})\,(\widetilde{\mathbf{B}}_p\widetilde{\mathbf{A}}_p - \mathbf{I})\nabla\widehat{u}\cdot\widetilde{\mathbf{A}}_p\nabla\widehat{u}\,d\widehat{x} + \int_\Omega (b_{33}\psi(x)^2 + 2(\mathbf{b}_3\cdot\widetilde{\mathbf{A}}_p\nabla\widehat{u})\psi(x))\,dx\,,$$

where $\mathbf{I}$ is the identity (2×2)-matrix. It is interesting to note that the first integral in (4.12) represents the error in averaging the coefficient matrix $\mathbf{A}(x)$; this becomes fully transparent in the case of a block-diagonal matrix $\mathbf{A}$, i.e., when $a_{31} = a_{32} = 0$ (then $\mathbf{B}_p = \mathbf{A}_p^{-1}$ and, without the averaging, the integral would be identically zero).

The functional M_2^2 of (4.1) also can be rearranged if one takes y^* as in (4.4). First, note that

$$\operatorname{Div} y^* = \operatorname{div}\widetilde{\mathbf{A}}_p\nabla\widehat{u} + \frac{\partial\psi}{\partial x_3}\,.$$

From (3.5) one can deduce

$$\operatorname{div}\widetilde{\mathbf{A}}_p\nabla\widehat{u} = -\widehat{f} - \frac{\nabla d}{d}\cdot\widetilde{\mathbf{A}}_p\nabla\widehat{u}\,.$$

Hence,

(4.13)
$$M_2^2 = \left\| f - \widetilde{f} - \frac{\widehat{F}_\ominus\sqrt{1+|\nabla d_\ominus|^2} + \widehat{F}_\oplus\sqrt{1+|\nabla d_\oplus|^2}}{d} - \frac{\nabla d}{d}\cdot\widetilde{\mathbf{A}}_p\nabla\widehat{u} + \frac{\partial\psi}{\partial x_3}\right\|^2_{L_2(\Omega)}\,.$$

The term M_3^2 with y^* from (4.4) reads

(4.14)
$$M_3^2 = \|F_\ominus - \widetilde{\mathbf{A}}_p\nabla\widehat{u}\cdot\boldsymbol{\nu}_\ominus - \psi\nu_{\ominus 3}\|^2_{L_2(\Gamma_\ominus)} + \|F_\oplus - \widetilde{\mathbf{A}}_p\nabla\widehat{u}\cdot\boldsymbol{\nu}_\oplus - \psi\nu_{\oplus 3}\|^2_{L_2(\Gamma_\oplus)}\,,$$

where $\widetilde{\mathbf{A}}_p\nabla\widehat{u}$ is considered as a vector in $\mathbb{R}^3$ with the third component equal to zero, and

$$\nu_{\ominus 3} = \frac{-1}{\sqrt{1+|\nabla d_\ominus|^2}}\,,\quad \nu_{\oplus 3} = \frac{1}{\sqrt{1+|\nabla d_\oplus|^2}}$$

are the third components of the normal vectors $\boldsymbol{\nu}_\ominus$ and $\boldsymbol{\nu}_\oplus$.

Now we can write the general a posteriori estimate for dimension reduction error as follows.

For all $\gamma > 0$ and $\delta > 0$ there holds

(4.15)
$$|||u-\widehat{u}|||^2 \le (1+\gamma)\,M_1^2 + \left(1+\frac{1}{\gamma}\right)(1+\delta)\,C_\Omega^2\,M_2^2 + \left(1+\frac{1}{\gamma}\right)\left(1+\frac{1}{\delta}\right)C_\Gamma^2(1+C_\Omega^2)\,M_3^2\,,$$

where the constants C_Ω and C_Γ are as above (see (4.2) and (4.3)) and the functionals M_1^2, M_2^2, and M_3^2 are given by (4.12), (4.13), and (4.14).

In estimate (4.15) we still have the freedom of choosing the auxiliary function ψ. The simplest choice is to take such a ψ so that the term M_3 (i.e., the residual on the

Neumann boundary condition) would be identically zero. To do so, we first rewrite the L_2-norms on $\Gamma_{\oplus,\ominus}$ in (4.14) as the integrals over $\widehat{\Omega}$:

$$\begin{aligned}&\| F_{\ominus} - \widetilde{\mathbf{A}}_p \nabla \widehat{u} \cdot \boldsymbol{\nu}_{\ominus} - \psi \nu_{\ominus 3} \|^2_{L_2(\Gamma_{\ominus})} \\ &\quad = \int_{\widehat{\Omega}} (\widehat{F}_{\ominus}(\widehat{x}) - \widetilde{\mathbf{A}}_p \nabla \widehat{u} \cdot \boldsymbol{\nu}_{\ominus} - \psi(\widehat{x}, d_{\ominus}(\widehat{x})) \nu_{\ominus 3})^2 \sqrt{1 + |\nabla d_{\ominus}|^2}\, d\widehat{x}\end{aligned}$$

(analogously for the norm in $L_2(\Gamma_{\oplus})$). Then, we denote

$$\widehat{G}_{\oplus,\ominus} := \widehat{F}_{\oplus,\ominus} - \widetilde{\mathbf{A}}_p \nabla \widehat{u} \cdot \boldsymbol{\nu}_{\oplus,\ominus}$$

and set

$$\psi_1(x) = \widehat{\alpha}(\widehat{x})\, x_3 + \widehat{\beta}(\widehat{x})\,, \tag{4.16}$$

where the functions $\widehat{\alpha}$ and $\widehat{\beta}$ ($\widehat{\alpha}\,,\, \widehat{\beta} \in L_2(\widehat{\Omega})$) are chosen so that

$$\psi_1 \nu_{\oplus 3} = \widehat{G}_{\oplus} \;\text{ at }\; x_3 = d_{\oplus}\,, \quad \psi_1 \nu_{\ominus 3} = \widehat{G}_{\ominus} \;\text{ at }\; x_3 = d_{\ominus}\,. \tag{4.17}$$

As $\nu_{\ominus 3}$, $\nu_{\oplus 3}$ belong to $L_\infty(\widehat{\Omega})$ and cannot be zero in $\widehat{\Omega}$, the functions $\widehat{\alpha}$ and $\widehat{\beta}$ are uniquely defined by conditions (4.17):

$$\widehat{\alpha} = \frac{1}{d}\left(\frac{\widehat{G}_{\oplus}}{\nu_{\oplus 3}} - \frac{\widehat{G}_{\ominus}}{\nu_{\ominus 3}}\right), \tag{4.18}$$

$$\widehat{\beta} = \frac{1}{d}\left(\frac{\widehat{G}_{\ominus}}{\nu_{\ominus 3}}\, d_{\oplus} - \frac{\widehat{G}_{\oplus}}{\nu_{\oplus 3}}\, d_{\ominus}\right). \tag{4.19}$$

It is obvious that the function ψ_1, as well as its derivative in the x_3-direction, belongs to $L_2(\Omega)$, and ψ_1 belongs to $L_2(\Gamma_{\oplus})$ and $L_2(\Gamma_{\ominus})$ (since $\psi_1\big|_{x_3 = d_{\oplus,\ominus}(\widehat{x})} \in L_2(\widehat{\Omega})$). Moreover, with such a function ψ the term M_3 becomes zero.

Remark 4.3. One can also consider a quadratic (with respect to x_3) function

$$\psi_2(x) = \psi_1(x) + \widehat{\eta}(\widehat{x})(x_3 - d_{\oplus}(\widehat{x}))(x_3 - d_{\ominus}(\widehat{x}))$$

with $\widehat{\eta}$ being an arbitrary function from $L_2(\widehat{\Omega})$. The substitution of ψ_2 instead of ψ into (4.14) will evidently imply $M_3 = 0$. In the second numerical example of section 6 we will use ψ_2 because of the freedom in the choice of the function $\widehat{\eta}$. It is clear that one can quite analogously construct the functions $\{\psi_m\}$, $m = 3, 4, \dots$, which would make the M_3-term vanish and could, possibly, allow us to approximate the third component of the exact flux $\mathbf{A}\nabla u$ with a higher accuracy.

Having chosen the function ψ such that $M_3 = 0$, one can obtain from (4.15) the following estimate for the squared energy norm of the modeling error:

$$|||u - \widehat{u}|||^2 \le (1 + \gamma)\, M_1^2 + \left(1 + \frac{1}{\gamma}\right) C_\Omega^2\, M_2^2\,, \tag{4.20}$$

where γ is any positive number, C_Ω is the Friedrichs constant, and M_1^2 and M_2^2 are given by (4.12) and (4.13). Minimizing the right-hand side of (4.20) with respect to the scalar parameter $\gamma > 0$, we immediately arrive at the estimate for the energy norm of the modeling error,

$$|||u - \widehat{u}||| \le M := M_1 + C_\Omega\, M_2, \tag{4.21}$$

with M_1 and M_2 defined by (4.12) and (4.13).

The rest of the paper will be devoted to the analysis of the properties of estimates (4.20), (4.21).

5. Particular cases. The error majorant M in (4.21) has been derived for quite general geometry of Ω and coefficient matrix $\mathbf{A}(x)$; to make the estimate more transparent, we consider two particular cases.

5.1. Plate of constant thickness. We assume that

$$d_\oplus = d_\ominus + d_0 \quad (d_0 = \text{const} > 0) \tag{5.1}$$

and, in addition, that

$$\mathbf{A} = \mathbf{A}(\widehat{x}) \ \text{ (this immediately implies } \mathbf{B} = \mathbf{B}(\widehat{x})\text{)}, \tag{5.2}$$

$$a_{31} = a_{32} = 0 \ \text{ (this yields } \mathbf{B}_p = \mathbf{A}_p^{-1},\ b_{33} = a_{33}^{-1},\ b_{31} = b_{32} = 0\text{)}. \tag{5.3}$$

With these assumptions and the choice $\psi = \psi_1$ (see (4.16)) the terms M_1 and M_2 in estimate (4.21) become simpler:

$$M_1 = \left(\int_\Omega a_{33}^{-1} \psi_1^2 \, dx \right)^{1/2}, \quad M_2 = \|f - \widetilde{f}\|_{L_2(\Omega)}. \tag{5.4}$$

One may notice that the integral in the first term M_1 of the error majorant M can be rewritten as

$$\int_\Omega a_{33}^{-1} \psi_1^2 \, dx = d_0 \cdot \int_{\widehat{\Omega}} a_{33}^{-1} \left(\widehat{\alpha}^2 \frac{d_\oplus^2 + d_\oplus d_\ominus + d_\ominus^2}{3} + \widehat{\alpha}\widehat{\beta}(d_\oplus + d_\ominus) + \widehat{\beta}^2 \right) d\widehat{x},$$

which means that the term M_1 is of order $\mathcal{O}(d_0^{1/2})$ when the plate thickness d_0 tends to zero. If $f \in L_\infty(\Omega)$, the second term M_2 is obviously of the same order $\mathcal{O}(d_0^{1/2})$; i.e., the whole estimator M converges to zero with the rate $\mathcal{O}(d_0^{1/2})$ as $d_0 \to 0$. This is the optimal convergence rate for the modeling error e in the energy norm, as was shown in [14] for the simpler case of a plate with plane parallel faces and $f = 0$ (see Remark 3.2). It is worth noting that, if $f \in C^1(\Omega)$, the second term in M is of higher order $\mathcal{O}(d_0^{3/2})$ as compared to the first term.

5.2. Plate with plane parallel faces. If in addition to (5.2), (5.3) we strengthen assumption (5.1) by replacing it with

$$d_\oplus = \frac{d_0}{2},\ d_\ominus = -\frac{d_0}{2} \quad (d_0 = \text{const} > 0), \tag{5.5}$$

then the function ψ_1 takes the simple form

$$\psi_1(x) = \frac{\widehat{F}_\oplus(\widehat{x}) + \widehat{F}_\ominus(\widehat{x})}{d_0} \, x_3 + \frac{\widehat{F}_\oplus(\widehat{x}) - \widehat{F}_\ominus(\widehat{x})}{2}$$

and the error estimate (4.21) reduces to

$$|||u - \widehat{u}||| \le \sqrt{\frac{d_0}{3}} \left(\int_{\widehat{\Omega}} a_{33}^{-1} (\widehat{F}_\oplus^2 + \widehat{F}_\ominus^2 - \widehat{F}_\oplus \widehat{F}_\ominus) \, d\widehat{x} \right)^{1/2} + C_\Omega \, \|f - \widetilde{f}\|_{L_2(\Omega)}. \tag{5.6}$$

If we set here $f = 0$, $a_{33} = 1$, and $\widehat{F}_\oplus = \widehat{F}_\ominus = \widehat{F}$, we obtain

$$|||u - \widehat{u}||| \le \sqrt{\frac{d_0}{3}} \, \|\widehat{F}\|_{L_2(\widehat{\Omega})}, \tag{5.7}$$

which is exactly the estimator of Babuška and Schwab (see [2]) for the zero-order reduced model. Thus, the latter estimator can be obtained as a particular case of the error majorant (4.21) if one makes the assumptions (5.2), (5.3), (5.5) and sets $f = 0$. This fact is especially interesting, since we advocate the estimation approach (see the details in [10]) that is completely different from the one utilized in [2].

Remark 5.1. The error estimate (4.21) contains the Friedrichs constant C_Ω that must be, in general, evaluated numerically. The constant depends solely on the geometry of the domain Ω and can be computed as $1/\sqrt{\lambda}$, where λ is the minimal eigenvalue of the elliptic operator $-\mathrm{Div}\,(\mathbf{A}\nabla\cdot\,)$ equipped with the homogeneous Dirichlet condition on Γ_0 and homogeneous Neumann conditions on $\Gamma_{\oplus,\ominus}$ (see (4.2)). It is clear that, in the case of a plate with plane parallel faces, C_Ω can be easily estimated from above if one computes the Friedrichs constant in a larger domain obtained by embedding the cross section $\widehat{\Omega}$ of Ω into some rectangle; the faces of this larger domain are then obtained by the extension of plane faces of Ω. Yet a simpler, but rougher, upper estimate for C_Ω in the case of a plate with plane parallel faces is given by $(\mathrm{diam}\,\widehat{\Omega})/c$, where c is the lower bound of the minimal eigenvalue of the matrix $\mathbf{A}(x)$ in Ω (see (2.6)). It is worth noticing that the constant C_Ω multiplies in the majorant the term M_2, which is often of higher order as compared to the first term M_1 (it is so, for example, in the particular cases considered above, when the function f is smooth). Then, the possible error of overestimation of C_Ω is harmless for the majorant accuracy.

6. Numerical examples.

6.1. Numerical test 1. In order to analyze the performance of the proposed error estimator, we consider a two-dimensional test problem in the "sine-shape" domain (see Figure 2 (left)) whose upper and lower faces are given by

$$d_{\oplus,\ominus}(x) = \sin(k\pi x) \pm \frac{d_0}{2}\,, \quad k = 1, 2, \dots\,,$$

where $d_0 > 0$ is the domain thickness. In this example, $\widehat{\Omega} = (0, 1)$ and $\Omega = \{(x, y) \in \mathbb{R}^2 \mid x \in \widehat{\Omega}\,,\ d_\ominus(x) < y < d_\oplus(x)\}$. The considered problem is

$$\begin{aligned} -\Delta u &= f && \text{in } \Omega\,,\\ u &= 0 && \text{at } x = 0 \text{ and } x = 1\,,\\ \nabla u \cdot \boldsymbol{\nu}_{\oplus,\ominus} &= F_{\oplus,\ominus} && \text{at } y = d_{\oplus,\ominus}\,, \end{aligned}$$

and the right-hand sides of the equation and of the boundary condition are computed using the exact solution

$$u(x, y) = \sin(\pi x) \cdot y^m \quad (m = 1, 2, \dots).$$

The reduced problem (3.3) is, in this case, a one-dimensional Dirichlet problem that, of course, can be solved very accurately (in the present work, we address the estimation of the modeling error only, assuming that the discretization error stemming from the solution of the reduced problem is negligible). The Friedrichs constant C_Ω was evaluated by computing the minimal eigenvalue of the Laplace operator with the corresponding homogeneous Dirichlet/Neumann boundary conditions (see Remark 5.1). We found that, for each $k = 1, 2, \dots$, C_Ω is an increasing function of the thickness d_0 as $d_0 \to 0$. There always exists, however, a clear upper bound for C_Ω; in particular, the estimates $C_\Omega \le \sqrt{2}$ for $k = 2$ and $C_\Omega \le 3$ for $k = 4$ hold true.

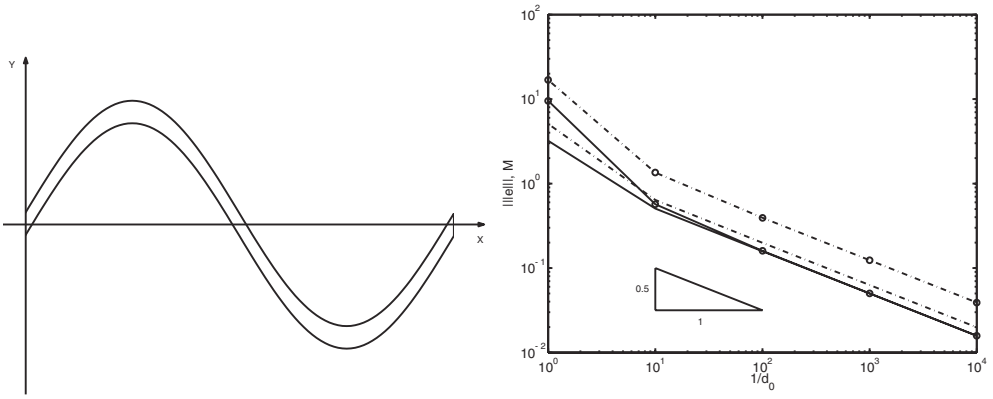

FIG. 2. *Left: The domain geometry. Right: Convergence rate of the exact modeling error and of the error majorant, $k = 2$, $m = 4$ (solid lines) and $m = 5$ (dash-dot lines). The majorant is indicated by "$\circ$."*

TABLE 1

Convergence of the exact modeling error in the energy norm ($|||e|||$) and of the error majorant (M) as $d_0 \to 0$ ($k = 2$); the results are rounded up to 10^{-4}.

d_0^{-1}	$m = 4$			$m = 5$		
	$\|\|\|e\|\|\|$	M	$\frac{M}{\|\|\|e\|\|\|}$	$\|\|\|e\|\|\|$	M	$\frac{M}{\|\|\|e\|\|\|}$
10^0	3.2108	9.5598	2.9774	5.0842	16.8434	3.3129
10^1	0.5058	0.5690	1.1250	0.6399	1.3481	2.1066
10^2	0.1581	0.1598	1.0106	0.1991	0.3937	1.9770
10^3	0.0500	0.0501	1.0010	0.0630	0.1237	1.9650
10^4	0.0158	0.0158	1.0000	0.0199	0.0391	1.9638

Figure 2 (right) shows the convergence rates of the exact modeling error in the energy norm ($|||e|||$) and of the error majorant (M) as the domain thickness d_0 tends to zero (the analysis here corresponds to the case $k = 2$, when the domain Ω has the shape depicted in Figure 2 (left)). It is clear that both the exact error and the majorant vanish with the theoretically predicted, optimal rate $\mathcal{O}(d_0^{1/2})$. However, the behavior of the majorant is different for even and odd values of degree m determining the polynomial growth of the exact solution u in the y-direction. The typical picture corresponding to an even value of the parameter m is well represented by the case $m = 4$ in Figure 2 (right); in this case, the majorant M demonstrates the asymptotic exactness, and, moreover, the *effectivity index* $\frac{M}{|||e|||}$ behaves like $1 + \mathcal{O}(d_0)$ (see Table 1). In the case of an odd value of m (represented by $m = 5$ in Figure 2 (right)), the majorant loses the property of asymptotic exactness, although the effectivity index remains stable and behaves, approximately, like $1.963 + \mathcal{O}(d_0)$ (see Table 1). This problem was addressed in Remark 4.1 and is caused by the fact that the approximate flux computed in the reduced model does not provide sufficient information on the corresponding components of the exact flux. We may note, however, that the effectivity index is still quite acceptable in this case. Finally, it is worth noticing that the presented error estimator provides a reliable upper bound for the exact error at any positive values of the domain thickness d_0, i.e., also in the cases when the domain is not "thin" at all.

The local error distributions provided by the exact error and by the first M_1-term of the majorant M (see (5.4)) are depicted in Figure 3 (here we consider the

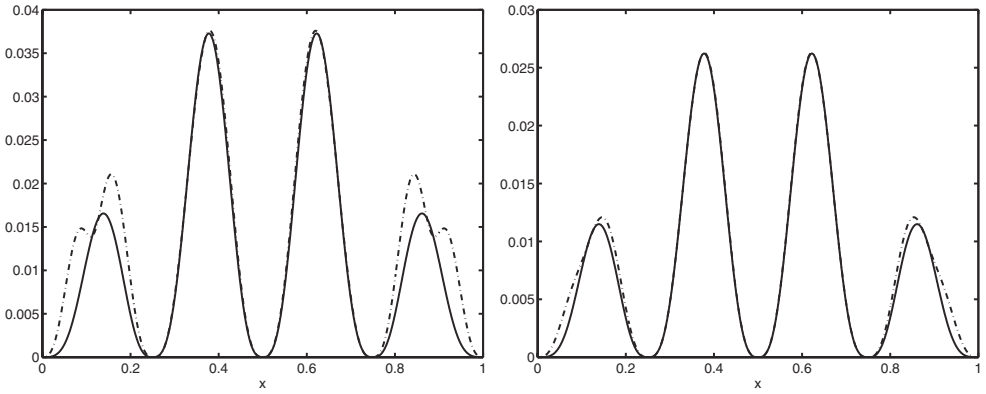

FIG. 3. *Local error distribution provided by the exact modeling error (solid line) and by the M_1-term of the majorant (dash-dot line), $k = 4$, $m = 4$. Left: $d_0 = 0.1$. Right: $d_0 = 0.05$.*

case $k = 4$, when the functions $d_{\oplus,\ominus}$ defining the shape of the domain have 4 extrema). The figure shows that already for rather large values of the domain thickness $d_0 = 0.1$ the majorant delivers sufficiently accurate information on the location of the regions of the biggest modeling error, while for $d_0 = 0.05$ the exact and the estimated error distributions are practically coincident.

6.2. Numerical test 2. The previous test shows that in the standard situations the proposed error estimator performs well. The example in this section demonstrates the performance of the estimator in a relatively difficult case when the right-hand side of the equation grows infinitely as the domain thickness tends to zero.

In this test, we consider a very simple geometry (see Figure 4 (left)), namely

$$d_{\oplus,\ominus} = \pm\frac{d_0}{2}\,,$$

where $d_0 > 0$ is the given thickness of the domain, $\widehat{\Omega} = (0,1)$ and $\Omega = \{(x,y) \in \mathbb{R}^2 \mid x \in \widehat{\Omega}\,,\ -\frac{d_0}{2} < y < \frac{d_0}{2}\}$. The considered problem reads

$$\begin{aligned} -\Delta u &= f && \text{in } \Omega\,,\\ u &= 0 && \text{at } x = 0 \text{ and } x = 1\,,\\ \frac{\partial u}{\partial y} &= \pm F_{\oplus,\ominus} && \text{at } y = \pm\frac{d_0}{2}\,, \end{aligned}$$

and the right-hand sides of the equation and of the boundary condition are computed using the exact solution

$$u(x,y) = \sin(\pi x)\cdot\frac{y^m}{d_0^{m-1}} \quad (m = 1, 2, \dots).$$

The scaling factor d_0^{m-1} makes this test essentially different from the previous one: while the Neumann boundary data $F_{\oplus,\ominus}$ remain of order $\mathcal{O}(1)$ as $d_0 \to 0$, the right-hand side of the equation f exhibits the behavior $f \sim \mathcal{O}(d_0)+\mathcal{O}\big(\frac{1}{d_0}\big)$, i.e., unboundedly grows when d_0 tends to zero. The unbounded growth of f may yield serious problems for an a posteriori error estimator, as we are about to see. We also note that the

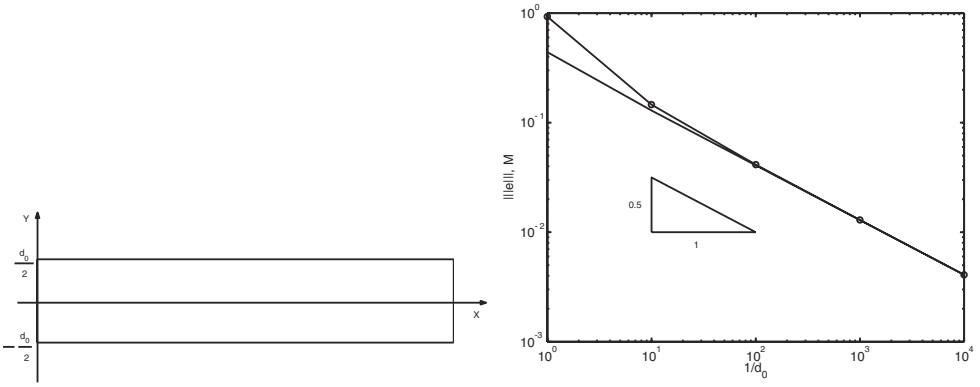

FIG. 4. *Left: The domain geometry. Right: Convergence rate of the exact modeling error and of the error majorant, $m = 2$; the majorant is indicated by* "$\circ$."

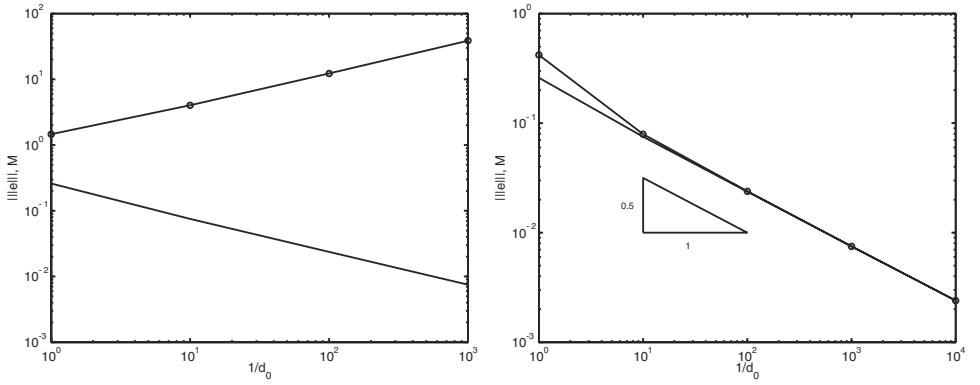

FIG. 5. *The case $m = 3$. Left: Divergence of the majorant $M(\psi_1)$ as $d_0 \to 0$. Right: Convergence of the improved majorant $M(\psi_2)$.*

constant C_Ω can be computed exactly in this example: $C_\Omega = \frac{1}{\pi}$ for all values of the thickness d_0.

First, we take $m = 2$ and observe the convergence of the exact modeling error in the energy norm and of the error majorant as d_0 tends to zero; see Figure 4 (right). As in the preceding example, the error majorant provides a reliable upper bound for the exact error at any values of the thickness d_0, both the exact error and the majorant demonstrate the optimal convergence rate $\mathcal{O}(d_0^{1/2})$ and, moreover, the error majorant shows the asymptotic exactness in this case (the effectivity index $\frac{M}{|||e|||} = 1 + \mathcal{O}(d_0)$; see the column under "$m = 2$, $M(\psi_1)$," in Table 2). However, if we set $m = 3$, the second term of the majorant M (i.e., $\|f - \widetilde{f}\|_{L_2(\Omega)}$, see (5.6)) becomes dominant and the whole estimator grows unboundedly, as can be seen in Figure 5 (left). The estimator becomes, of course, useless as it dramatically overestimates the exact error for small values of d_0. It is rather clear that the problem originates from the poor choice of the auxiliary function ψ that is supposed to approximate $\frac{\partial u}{\partial y}$; for $m = 3$ the derivative is quadratic and cannot be adequately represented by the linear function ψ_1.

The situation may be improved by invoking the quadratic function $\psi = \psi_2$ (see Remark 4.3), $\psi_2(x,y) = \psi_1(x,y) + \widehat{\eta}(x)\,(y^2 - \frac{d_0^2}{4})$, where $\widehat{\eta}$ is an arbitrary function from $L_2(\widehat{\Omega})$. The possibility of choosing a suitable $\widehat{\eta}$ enables us to suppress the unbounded growth of f in the M_2-term of the majorant and makes the majorant flexible enough to efficiently reproduce the behavior of the exact error.

If we plug ψ_2 into the estimate (4.20), we obtain

$$|||u - \widehat{u}|||^2 \le M^2(\widehat{\eta}, \gamma) \qquad \forall \widehat{\eta} \in L_2(\widehat{\Omega})\,,\ \forall \gamma > 0\,, \tag{6.1}$$

where

$$\begin{aligned} M^2(\widehat{\eta},\gamma) :&= (1+\gamma)\|\psi_2\|^2_{L_2(\Omega)} + \left(1 + \frac{1}{\gamma}\right) C_\Omega^2 \left\| f - \widetilde{f} + \frac{\partial \psi_2}{\partial y} \right\|^2_{L_2(\Omega)} \\ &= (1+\gamma) \int_\Omega \left(\psi_1(x,y) + \widehat{\eta}(x)\,\left(y^2 - \frac{d_0^2}{4}\right)\right)^2 dxdy \\ &\quad + \left(1 + \frac{1}{\gamma}\right) C_\Omega^2 \int_\Omega (f(x,y) - \widetilde{f}(x) + \widehat{\eta}(x)\cdot 2y)^2\, dxdy\,. \end{aligned}$$

Since estimate (6.1) is valid for any $\gamma > 0$ and $\widehat{\eta}$ from $L_2(\widehat{\Omega})$, one can minimize the functional $M^2(\widehat{\eta},\gamma)$ with respect to these parameters. In particular, one can set $\gamma = \gamma_* < 1$ (the concrete value of γ_* does not matter, as the numerical experiments show; we used the value $\gamma_* = 0.5$) and find $\widehat{\eta}_{\min}$ as the minimizer of $M^2(\widehat{\eta},\gamma_*)$ over the space S of piecewise-constant functions defined on some finite subdivision of $\widehat{\Omega}$ (obviously, $S \subset L_2(\widehat{\Omega})$). The minimization problem is just an L_2-projection onto the space of functions defined on $\widehat{\Omega}$ and amounts to the solution of a linear system with the diagonal matrix.

The properties of the improved majorant $M(\psi_2) = M_1(\psi_2) + C_\Omega\, M_2(\psi_2)$, where

$$\begin{aligned} M_1(\psi_2) &:= \left\| \psi_1 + \widehat{\eta}_{\min}\,\left(y^2 - \frac{d_0^2}{4}\right) \right\|_{L_2(\Omega)}, \\ M_2(\psi_2) &:= \|f - \widetilde{f} + \widehat{\eta}_{\min}\cdot 2y\|_{L_2(\Omega)}, \end{aligned}$$

can be observed in Figure 5 (right). We see that the improved majorant vanishes with the optimal rate $\mathcal{O}(d_0^{1/2})$ as $d_0 \to 0$, remains a reliable upper bound for the exact error at any values of the thickness d_0, and even demonstrates the asymptotic exactness with the effectivity index behaving like $1 + \mathcal{O}(d_0)$ (see Table 2).

We may note that in the case of larger values of m ($m > 3$) the higher degree function ψ_{m-1} might be needed (see Remark 4.3); the function will contain several free parameters which are the functions from $L_2(\widehat{\Omega})$, and, hence, the minimization should be performed with respect to all of them. However, as this always remains a least-squares minimization problem, the total complexity for the moderate values of m will not be greater than the complexity of solving the reduced problem. In general, if the right-hand side f exhibits an unbounded growth for $d_0 \to 0$ and no a priori information on the behavior of the exact solution is available, one has to choose the function ψ in an adaptive way; i.e., starting with ψ_1, increase the polynomial degree of the function until the difference between the two successive majorants $M(\psi_{n-1})$ and $M(\psi_n)$ becomes small enough.

TABLE 2

Convergence of the exact modeling error in the energy norm ($|||e|||$) and of the error majorant (M) as $d_0 \to 0$; the results are rounded up to 10^{-4}.

d_0^{-1}	$m=2,\ M(\psi_1)$			$m=3,\ M(\psi_2)$		
	$\|\|\|e\|\|\|$	M	$\frac{M}{\|\|\|e\|\|\|}$	$\|\|\|e\|\|\|$	M	$\frac{M}{\|\|\|e\|\|\|}$
10^0	0.4405	0.9284	2.1074	0.2594	0.4187	1.6142
10^1	0.1291	0.1461	1.1265	0.0751	0.0793	1.0562
10^2	0.0408	0.0414	1.0127	0.0237	0.0239	1.0056
10^3	0.0129	0.0130	1.0013	0.0075	0.0076	1.0006
10^4	0.0041	0.0041	1.0001	0.0024	0.0024	1.0001

7. Conclusions. For the zero-order dimension reduction method, the new a posteriori error estimator has been derived in a general geometrical setting of the problem and without any specific assumptions on the given data. In particular, the estimator reduces to the Babuška–Schwab estimator when the physical domain Ω is a plate with plane parallel faces and the equation has zero right-hand side. It has been demonstrated, both theoretically and numerically, that also in a more complicated case of a plate having constant thickness but nonplane faces and for a general right-hand side $f \in L_\infty(\Omega)$ the proposed estimator vanishes with the optimal rate $\mathcal{O}(d_0^{1/2})$ as the plate thickness d_0 tends to zero. Since the estimator always provides an upper bound for the exact modeling error, the latter convergence result can be considered as the generalization of the result on the convergence of the dimension reduction error proved in [14] (see also [2]) for the case of a plate with plane parallel faces and zero right-hand side f.

The presented estimator cannot, however, be considered as just a generalization of the explicit residual-type error estimator to the case of more complicated geometry, coefficients, and right-hand side. As numerical test 2 shows, in the problem with the right-hand side f infinitely growing as the plate thickness tends to zero, some additional "degree of freedom" should be introduced into the estimator to suppress the unbounded growth of f. Thus, it seems that any error estimator that cannot be adjusted to the particular problem will fail in such a case. The proposed estimator is sufficiently flexible to allow the modification necessary for capturing the behavior of the exact error. The recovered efficiency of the estimator manifests itself in the asymptotics of the effectivity index $\frac{M}{|||e|||} = 1 + \mathcal{O}(d_0)$ when d_0 tends to zero. We have to note that such an asymptotics may not always be observed if the domain Ω has nonplane faces; however, even in the latter case, the effectivity index of the estimator remains stable (i.e., does not grow with the decreasing domain thickness) and stays at the acceptable level.

The computational cost of evaluating the presented error majorant is typically smaller than or, in the worst case, of the same order as the cost of solving the reduced, lower-dimensional problem. Finally, the numerical results show that the proposed estimator is capable of an accurate indication of the local error distribution and, hence, may be utilized not only for the verification of the dimensionally reduced model but also for its adaptive improvement.

REFERENCES

[1] M. AINSWORTH, *A posteriori error estimation for fully discrete hierarchic models of elliptic boundary value problems on thin domains*, Numer. Math., 80 (1998), pp. 325–362.

[2] I. BABUŠKA, I. LEE, AND C. SCHWAB, *On the a posteriori estimation of the modeling error for the heat conduction in a plate and its use for adaptive hierarchical modeling*, Appl. Numer. Math., 14 (1994), pp. 5–21.

[3] I. Babuška and C. Schwab, *A posteriori error estimation for hierarchic models of elliptic boundary value problems on thin domains*, SIAM J. Numer. Anal., 33 (1996), pp. 221–246.
[4] P. Ladeveze and D. Leguillon, *Error estimate procedure in the finite element method and applications*, SIAM J. Numer. Anal., 20 (1983), pp. 485–509.
[5] J. T. Oden and J. R. Cho, *Adaptive* hpq*-finite element methods of hierarchical models for plate- and shell-like structures*, Comput. Methods Appl. Mech. Engrg., 136 (1996), pp. 317–345.
[6] W. Prager and J. L. Synge, *Approximations in elasticity based on the concept of function space*, Quart. Appl. Math., 5 (1947), pp. 241–269.
[7] S. I. Repin, *A posteriori error estimation for variational problems with uniformly convex functionals*, Math. Comp., 69 (2000), pp. 481–600.
[8] S. I. Repin, *Estimates for errors in two-dimensional models of elasticity theory*, J. Math. Sci. (New York), 106 (2001), pp. 3027–3041.
[9] S. I. Repin, S. A. Sauter, and A. A. Smolianski, *A posteriori error estimation for the Dirichlet problem with account of the error in the approximation of boundary conditions*, Computing, 70 (2003), pp. 205–233.
[10] S. I. Repin, S. A. Sauter, and A. A. Smolianski, *A posteriori error estimation for the Poisson equation with mixed Dirichlet/Neumann boundary conditions*, J. Comput. Appl. Math., 164/165 (2004), pp. 601–612.
[11] S. I. Repin, S. A. Sauter, and A. A. Smolianski, *A posteriori estimation of dimension reduction errors*, in Proceedings of the 5th European Conference on Numerical Mathematics and Advanced Applications, (ENUMATH 2003), Springer-Verlag, New York, 2004, to appear.
[12] E. Stein and S. Ohnimus, *Coupled model- and solution-adaptivity in the finite-element method*, Comput. Methods Appl. Mech. Engrg., 150 (1997), pp. 327–350.
[13] J. L. Synge, *The Hypercircle in Mathematical Physics*, Cambridge University Press, Cambridge, UK, 1957.
[14] M.Vogelius and I. Babuška, *On a dimensional reduction method* I. *The optimal selection of basis functions*, Math. Comp., 37 (1981), pp. 31–46.
[15] M.Vogelius and I. Babuška, *On a dimensional reduction method* III. *A posteriori error estimation and an adaptive approach*, Math. Comp., 37 (1981), pp. 361–384.